The Behaviour of the XMM-Newton Background: From the beginning of the mission until May 2023

XMM-SOC-GEN-TN-0014
issue 3.16

R. González-Riestra and P.M. Rodríguez-Pascual

XMM-SOC User Support Group

June 1, 2023

1 Introduction

This document supersedes XMM-SOC-USR-TN-0014, issue 3.15. The sample includes now data obtained until 1st May 2023.

The aim of this document is to describe the seasonal and long-term behaviour of the XMM-Newton background. For this purpose we have examined the background in RGS1 and EPIC-pn science observations taken from the beginning of the mission until May 2023.

The first version of this document, issued in January 2007, fulfilled the recommendation made by the XMM-Newton Users Group *"to reassess the EPIC background loading for a 1 year sample in order to investigate a seasonal dependence" (rec. 2006-05-19/34).*

The contributors to the EPIC and RGS background are detailed in the XMM Users Handbook and in the XMM-Newton Background Analysis page.

The most relevant features are:

The EPIC background has two components: a cosmic X-ray background, and an instrumental background. The latter can be further divided into a detector noise component (dominant below 200 eV) and a second component due to the interaction of particles with the structure surrounding the detectors and the detectors themselves. This component is particularly important above a few keV.

The particle induced background has in turn two components: a stable internal component, due to the interaction of high-energy particles (energies above some 100 MeV) with the structure surrounding the detectors and possibly the detectors themselves, and an external "flaring" component, characterised by strong and rapid variability. This flaring component is attributed to soft protons (with energies below a few 100 keV), which are presumably funnelled towards the detectors by the X-ray mirrors.

The RGS background has also several components, the dominant one being soft protons entering through the mirrors.

The current understanding is that soft protons are most likely organised in clouds populating the Earth's magnetosphere. The number of such clouds encountered by XMM-Newton in its orbit depends upon many factors, such as the altitude of the satellite, its position with respect to the magnetosphere, and the amount of solar activity.

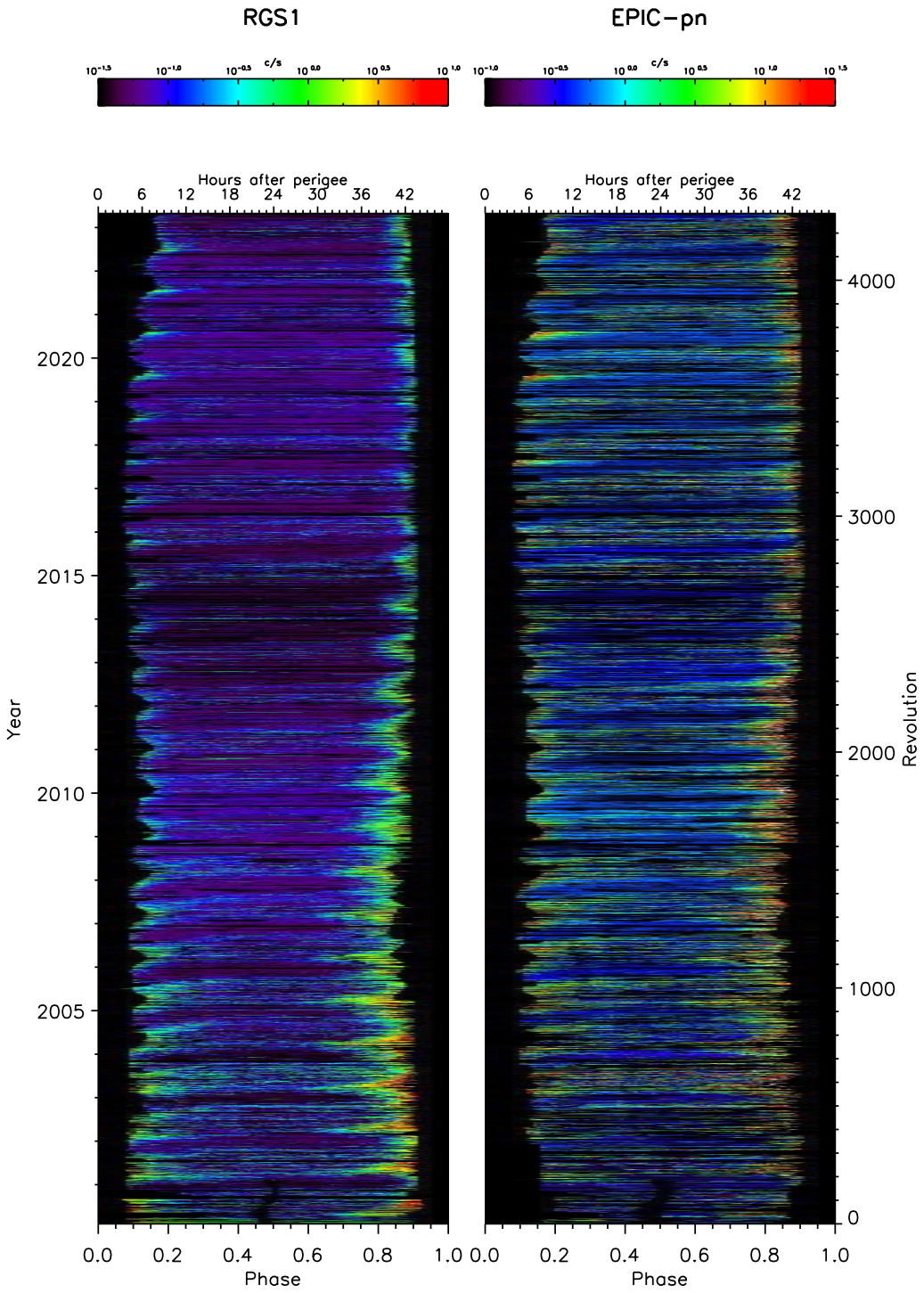

Figure 1: Evolution of the background in RGS (left) and EPIC-pn (right) since the beginning of the mission until May 2023. The selection criteria in Mode/Filter makes EPIC-pn data to be more scarce than RGS. In addition, EPIC-pn science exposures are generally stopped earlier than RGS exposures when approaching perigee passage.

2 Data Sample and Methodology

In this study we have used the following datasets:

- RGS[1]
  - RGS1 data since the beginning of the operational phase until 1st May 2023
  - Spectroscopy mode
  - Background indicator: countrate in CCD9 off axis region (> 1 arcmin away from the on-axis position)
    `(CCDNR==9 && (XDSP_CORR < -0.0003 || XDSP_CORR > 0.0003))`
- EPIC-pn
  - EPIC-pn data since the beginning of the operational phase until 1st May 2023
  - Full Frame or Extended Full Frame mode with THIN or MEDIUM filter.
  - Background indicator: high energy events
    `(FLAG==0) && (PI>10000) && (PATTERN==0)`

3 Mission Planning constraints and Operational Procedures

The Radiation Monitor (RM) on-board XMM-Newton is mainly used to detect the entry/exit to/from the Earth radiation belts. Whenever the RM flux is higher than a given threshold (*Radiation Monitor Warning Flag Active*) the EPIC-MOS cameras are kept closed or commanded to SAFE-STANDBY mode, EPIC-pn is commanded to IDLE mode with the CLOSED filter, and RGS is commanded to SETUP mode. The RM Warning Flag can also be set to "active" during solar flares, leading to the interruption of science observations.

Even before the limit for the RM Warning Flag goes to "active", high radiation (due either to proximity to perigee or to low-energy protons flares) can be identified with the information provided by the X-ray science instruments, basically the countrate in the EPIC-MOS peripheral CCDs, in RGS CCD9 and the EPIC-pn Discarded Lines.

In general, RGS is stopped at higher radiation levels than EPIC. For this reason RGS data have a more complete coverage of the end of the revolution.

Starting in April 2005, science observations at the beginning of the revolution are scheduled only in the time predicted as "low-radiation" in the model by Casale and Fauste (2004), as explained in the next paragraph.

EPIC-MOS observations with the CALCLOSED filter are scheduled at the beginning of the revolution if there are more than 3 ks between the start of the Science Window and the predicted end of the high radiation period. EPIC-pn CALCLOSED filter exposures are scheduled only if there are more than 6 ks available. The last science observation in the revolution is scheduled to last until the end of the Science Window, set at a fixed S/C altitude, and the EPIC and RGS instruments within this observation are stopped if needed when the radiation reaches the critical level. EPIC-MOS exposures with the CALCLOSED filter are then performed, if there is enough time available

4 Overall Trend

Fig. 1 shows the evolution of the background in RGS (left) and EPIC-pn (right). EPIC-pn data are more scarce due to the selection of mode and filter. Also, RGS is usually on for a longer time at the

[1]When we mention the 'RGS background' we refer, strictly speaking, to the 'RGS1 background', but any conclusion is equally valid for RGS2, as the backgrounds of both RGS instruments are totally correlated.

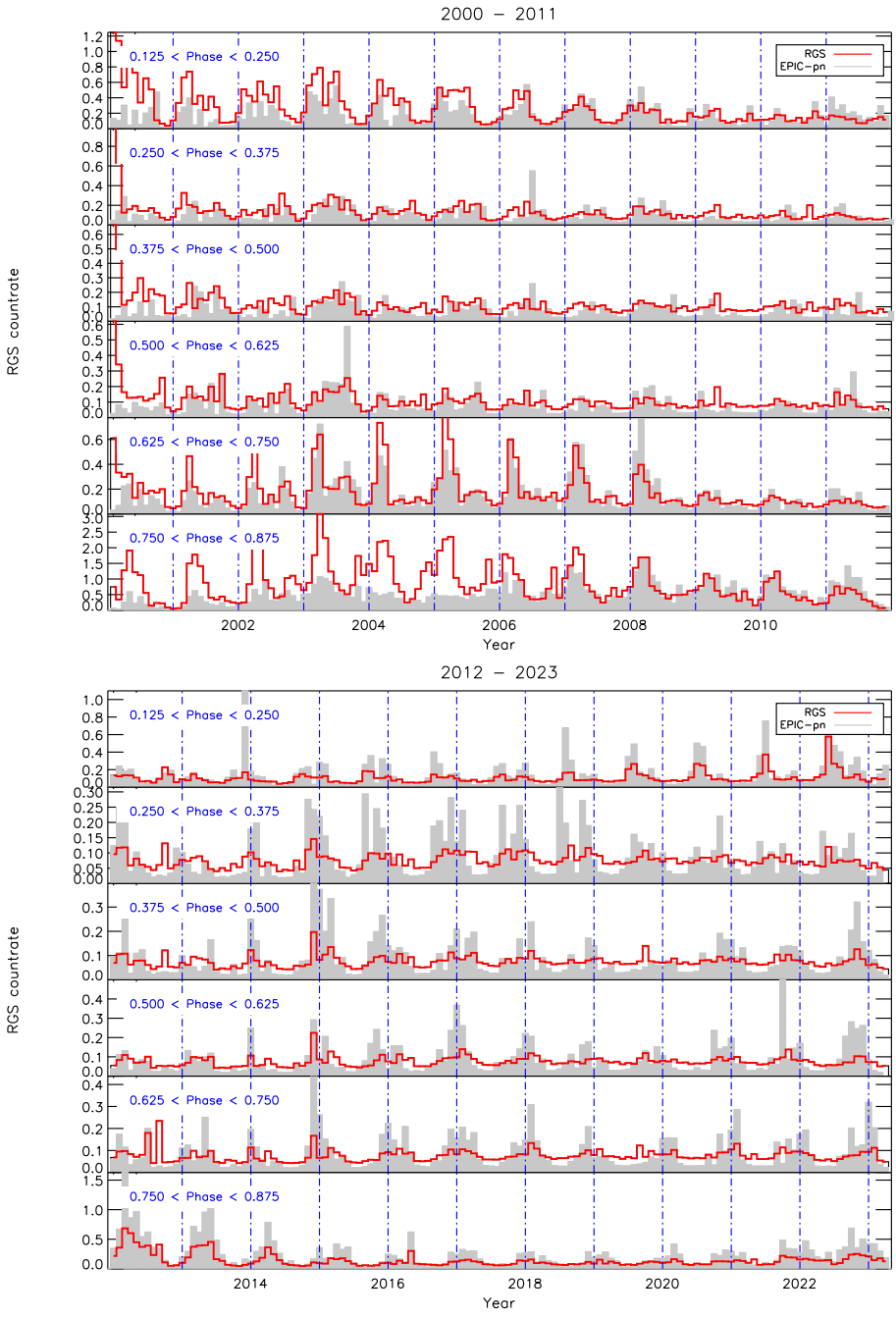

Figure 2: Evolution of the XMM-Newton background along the years in different parts of the revolution (top: until end 2011, bottom: from 2012 until May 2023). Data have been averaged in one month bins. RGS is shown in red and EPIC-pn in grey. EPIC-pn countrates have been arbitrarily scaled for clarity. Note the different scales in each panel.

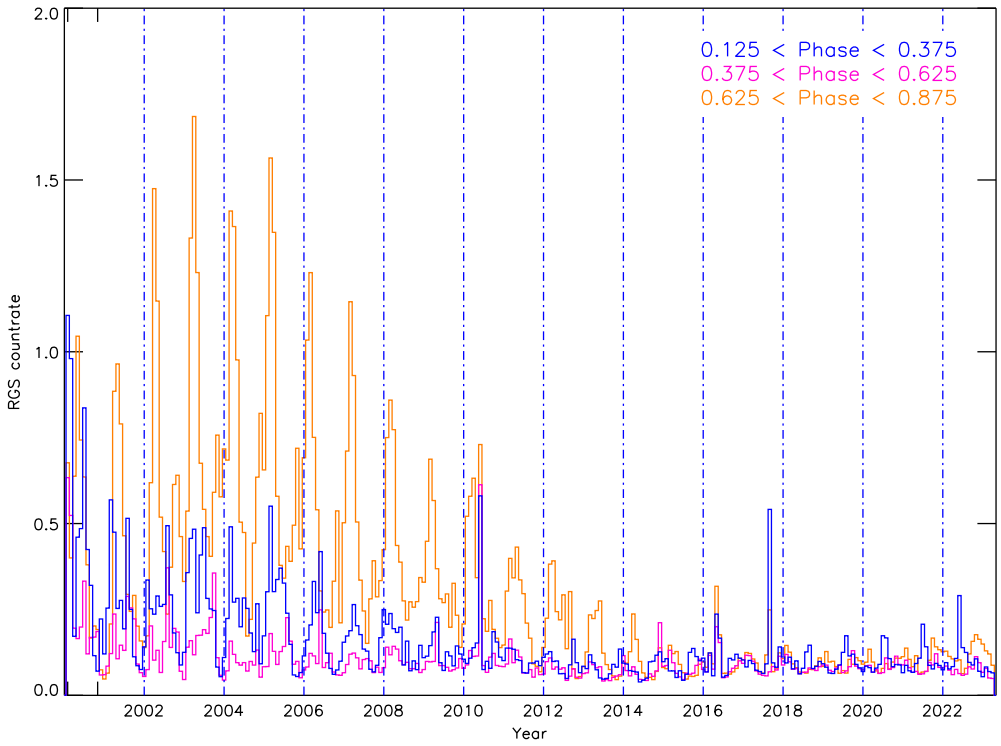

Figure 3: Similar to Fig. 2, but showing all the data with the same scale. Data have been averaged in one month bins.

end of the revolution. As shown in the figure, within the intrinsic scatter in the data, there are not significant differences in the behaviour of the background in both instruments.

The change in start time of the first data in the revolution is mainly due to the prediction of the radiation model, that is used to schedule the the first science observation. On the other hand, the end time of the last data is mostly driven by the radiation behaviour itself, since no model is applied to stop the last observation: it is stopped either when the radiation goes high, or at a given S/C altitude.

In what follows, we have divided the revolution in six parts of four hours each, from phase 0.125 (six hour after perigee passage) to 0.875 (six hours before perigee passage). We refer to the first two parts as the *beginning of the revolution*, to the next two as the *apogee*, and to the remaining two as the *end of the revolution*.

5 Secular Variations

The evolution of the background along the mission is shown in Figs. 2 and 3. The general agreement in the behaviour of the background in both instruments justifies that we base our results mainly in the RGS data, due to the better coverage. The overall level of background has decreased slightly since the start of the mission. Also, the annual periodicity observed in the first years, though still present, is less pronounced now or has even disappeared.

The RGS background at apogee is shown in Fig. 4. In a period of high solar activity, until approximately 2006, the number of flares was larger and the minimum background was at a level of 0.03 cts/s. The level of the background started to increase in 2006, reaching a maximum in 2009, with the start of the solar cycle, with a minimum around 2013–2014 after which it started to increase again until 2020.

RGS countrate at apogee

Year	Rate ± std	Year	Rate ± std
2000	0.17 ± 0.10	2012	0.07 ± 0.02
2001	0.13 ± 0.06	2013	0.06 ± 0.02
2002	0.11 ± 0.05	2014	0.08 ± 0.03
2003	0.13 ± 0.06	2015	0.08 ± 0.03
2004	0.09 ± 0.03	2016	0.08 ± 0.02
2005	0.10 ± 0.04	2017	0.08 ± 0.02
2006	0.09 ± 0.03	2018	0.08 ± 0.01
2007	0.09 ± 0.03	2019	0.08 ± 0.02
2008	0.10 ± 0.04	2020	0.07 ± 0.01
2009	0.09 ± 0.03	2021	0.08 ± 0.02
2010	0.09 ± 0.03	2022	0.07 ± 0.02
2011	0.09 ± 0.03		

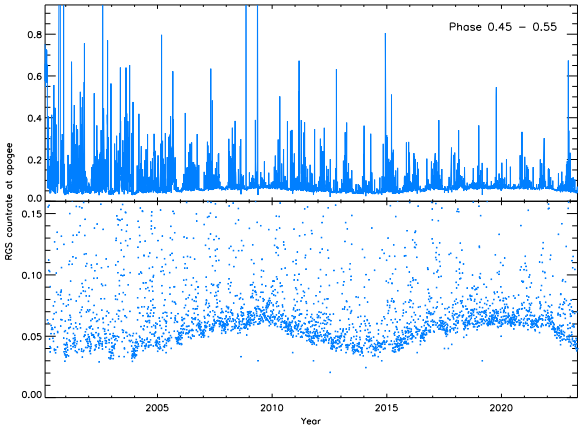

Figure 4: RGS background at apogee. As shown in the top panel, flares were stronger and more frequent during the first years of the mission. The lower panel presents the same data with a different scale, to better show that the *minimum* background was lower during the period of high solar activity, increased during the solar minimum, and decreased again until reaching a minimum in 2014. The level has rising in the last few years until reaching a maximum again in 2020. The table on the left lists the average yearly countrate around apogee.

6 Seasonal and Orbital Variations

Figs. 5 and 6 show the behaviour of the background along the year. Casale and Fauste (2004) have shown that the observed seasonal dependence can be explained by the asymmetry of the Earth magnetic field along the sunward-antisun line.

We have plotted in Fig. 5 separately four periods of time, to better show the changes in the characteristics of the seasonal variations.

a) **The beginning of the revolution**

Seasonal variations at the beginning of the revolution were more marked in the first years of the mission. In the last years the background is slightly lower from January to May, increasing in July-September.

b) **The apogee**

Since 2005, when it was slightly lower in December-January, the intensity of the RGS background close to apogee has not shown significant seasonal changes.

c) **The end of the revolution**

During the first ten years of the mission, the highest background levels and the largest seasonal variations were observed in the second half of the revolution, peaking around March, when the background was on average ≈ two times higher than in August. Such variations are not observed in the last years.

7 Conclusions

The results of this study are summarised in Table 1 and Figures 7 and 8. The table lists the monthly average RGS background countrate in the different parts of the revolution until 2005, from 2006 to 2011, from 2012 to 2017, and since 2018 until now (May 2023). Also listed are the standard deviations of each monthly average (i.e. the standard deviation of the monthly averages of the different years). Large standard deviations indicate large year-to-year variations in the given month.

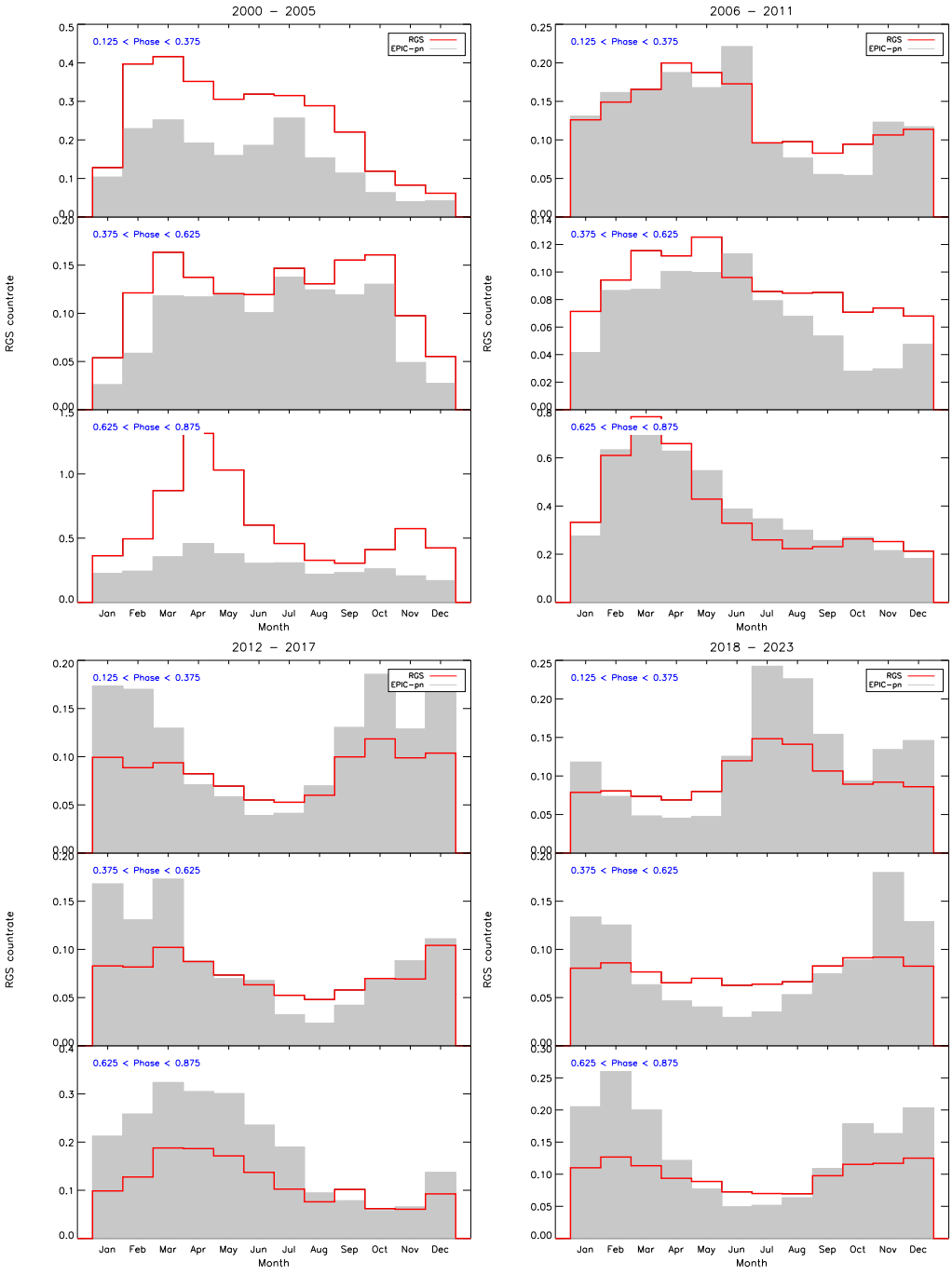

Figure 5: Behaviour of the monthly background in different parts of the revolution in four different periods along the mission. RGS is shown in red and EPIC-pn in grey. Units are RGS cts/s. EPIC-pn countrates have been arbitrarily scaled. Note the different scales in each panel.

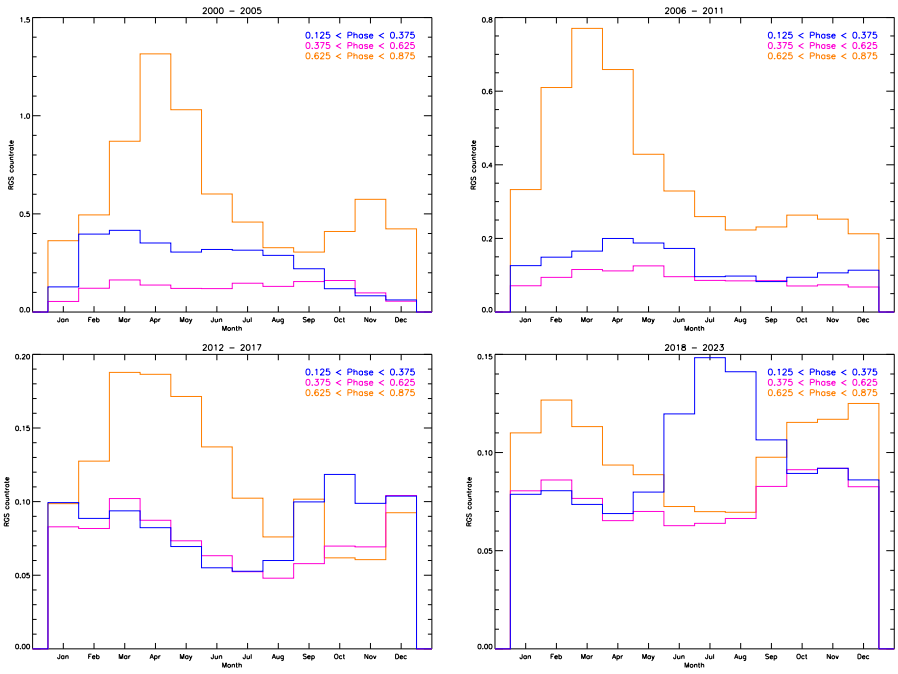

Figure 6: Similar to Fig. 5, but showing the monthly RGS background in different parts of the revolution with the same scale (until end 2004, from 2005 to end 2010, from 2011 to end 2016, and: since 2017. Note the different scales of the panels).

The conclusions listed below refer to the behaviour of the background in the last five years.

- The most remarkable characteristic is the change in the intensity of the background along the orbit. The distance to the Earth is the dominant factor (the background is lower close to apogee, as expected), but the asymmetry of the changes in the background when moving away from perigee and when approaching to it indicates that other effects may play an important role.
- Except in July-August, the background is lower at the beginning of the revolution than at the end. But even in that period, high background does not extend beyond orbital phase 0.2 ($\approx$ ten hours after perigee), and this only happens in July-August. The background starts to increase $\approx$ six hours before perigee.
- Seasonal variations are now much less pronounced than in the first years of the mission. At apogee, the background changes by less than a $\approx 20\%$ along the year. The variation is larger, up to a factor 2, at the end of the revolution. Even in the most favourable conditions, the background at the end of the revolution is higher than the highest value observed at apogee.
- Periods of high solar activity are characterised by frequent flares, but also by a lower background at apogee.

References

XMM-Newton Users Handbook

Attempt of Modelling the XMM-Newton Radiation Environment, XMM-OPS-TN-004, Casale, M. and Fauste, J., 2004.

Table 1: Average monthly RGS Background Countrate*

	Phase in Revolution / [Hours after Perigee]				
Month	0.125-0.250 [6-12]	0.250-0.375 [12-18]	0.375-0.625 [18-30]	0.625-0.750 [30-36]	0.750-0.875 [36-42]
2000 - 2005					
January	0.19 (0.05)	0.06 (0.01)	0.05 (0.02)	0.08 (0.07)	0.66 (0.60)
February	0.55 (0.34)	0.25 (0.34)	0.12 (0.23)	0.20 (0.20)	0.81 (0.67)
March	0.64 (0.26)	0.23 (0.19)	0.16 (0.12)	0.48 (0.24)	1.33 (0.92)
April	0.59 (0.17)	0.16 (0.04)	0.14 (0.05)	0.54 (0.12)	2.19 (0.66)
May	0.48 (0.21)	0.17 (0.03)	0.12 (0.03)	0.22 (0.09)	1.97 (0.45)
June	0.48 (0.15)	0.18 (0.09)	0.12 (0.04)	0.13 (0.05)	1.08 (0.26)
July	0.45 (0.18)	0.18 (0.06)	0.15 (0.04)	0.17 (0.06)	0.76 (0.22)
August	0.43 (0.14)	0.16 (0.03)	0.13 (0.04)	0.17 (0.07)	0.49 (0.18)
September	0.19 (0.15)	0.25 (0.05)	0.16 (0.04)	0.18 (0.07)	0.43 (0.17)
October	0.10 (0.04)	0.14 (0.04)	0.16 (0.05)	0.18 (0.04)	0.65 (0.29)
November	0.08 (0.03)	0.09 (0.02)	0.10 (0.06)	0.12 (0.04)	1.08 (0.65)
December	0.08 (0.02)	0.05 (0.01)	0.06 (0.01)	0.07 (0.01)	0.77 (0.54)
2006 - 2011					
January	0.17 (0.07)	0.09 (0.02)	0.07 (0.01)	0.09 (0.02)	0.61 (0.32)
February	0.20 (0.06)	0.11 (0.04)	0.09 (0.02)	0.18 (0.08)	1.07 (0.48)
March	0.21 (0.09)	0.13 (0.03)	0.12 (0.03)	0.32 (0.22)	1.32 (0.47)
April	0.28 (0.14)	0.13 (0.03)	0.11 (0.01)	0.23 (0.15)	1.18 (0.46)
May	0.24 (0.09)	0.13 (0.04)	0.13 (0.04)	0.15 (0.05)	0.74 (0.13)
June	0.22 (0.15)	0.12 (0.06)	0.10 (0.03)	0.11 (0.04)	0.54 (0.09)
July	0.10 (0.03)	0.09 (0.04)	0.09 (0.01)	0.10 (0.01)	0.45 (0.07)
August	0.10 (0.03)	0.09 (0.03)	0.08 (0.02)	0.10 (0.02)	0.37 (0.09)
September	0.09 (0.02)	0.08 (0.02)	0.09 (0.02)	0.10 (0.03)	0.39 (0.08)
October	0.10 (0.03)	0.09 (0.06)	0.07 (0.01)	0.10 (0.04)	0.46 (0.23)
November	0.15 (0.06)	0.06 (0.01)	0.07 (0.01)	0.09 (0.04)	0.43 (0.46)
December	0.16 (0.04)	0.07 (0.01)	0.07 (0.01)	0.07 (0.02)	0.36 (0.24)
2012 - 2017					
January	0.10 (0.02)	0.09 (0.01)	0.08 (0.02)	0.08 (0.02)	0.11 (0.05)
February	0.09 (0.03)	0.09 (0.02)	0.08 (0.02)	0.08 (0.02)	0.18 (0.10)
March	0.10 (0.04)	0.09 (0.02)	0.10 (0.02)	0.10 (0.02)	0.28 (0.21)
April	0.09 (0.03)	0.08 (0.02)	0.09 (0.01)	0.08 (0.01)	0.29 (0.20)
May	0.07 (0.02)	0.07 (0.01)	0.07 (0.01)	0.07 (0.01)	0.27 (0.13)
June	0.06 (0.01)	0.05 (0.01)	0.06 (0.01)	0.07 (0.02)	0.20 (0.16)
July	0.06 (0.01)	0.05 (0.01)	0.05 (0.01)	0.07 (0.05)	0.14 (0.13)
August	0.07 (0.03)	0.05 (0.01)	0.05 (0.01)	0.05 (0.01)	0.11 (0.07)
September	0.13 (0.04)	0.07 (0.01)	0.06 (0.01)	0.08 (0.07)	0.12 (0.14)
October	0.15 (0.06)	0.09 (0.03)	0.07 (0.01)	0.06 (0.01)	0.06 (0.02)
November	0.11 (0.02)	0.09 (0.03)	0.07 (0.02)	0.06 (0.01)	0.06 (0.01)
December	0.11 (0.04)	0.09 (0.03)	0.10 (0.06)	0.09 (0.04)	0.10 (0.03)
2018 - 2023					
January	0.08 (0.02)	0.08 (0.02)	0.08 (0.01)	0.09 (0.01)	0.13 (0.04)
February	0.08 (0.01)	0.08 (0.01)	0.09 (0.02)	0.11 (0.02)	0.15 (0.02)
March	0.08 (0.01)	0.07 (0.01)	0.08 (0.02)	0.08 (0.02)	0.14 (0.04)
April	0.08 (0.02)	0.06 (0.01)	0.07 (0.01)	0.07 (0.01)	0.12 (0.01)
May	0.09 (0.03)	0.07 (0.01)	0.07 (0.01)	0.07 (0.01)	0.11 (0.03)
June	0.16 (0.22)	0.08 (0.02)	0.06 (0.01)	0.06 (0.01)	0.08 (0.04)
July	0.24 (0.10)	0.07 (0.01)	0.06 (0.01)	0.06 (0.01)	0.08 (0.01)
August	0.22 (0.04)	0.08 (0.01)	0.07 (0.01)	0.06 (0.01)	0.08 (0.01)
September	0.13 (0.03)	0.09 (0.02)	0.08 (0.01)	0.09 (0.02)	0.11 (0.04)
October	0.10 (0.02)	0.08 (0.02)	0.09 (0.02)	0.08 (0.02)	0.15 (0.07)
November	0.10 (0.03)	0.08 (0.01)	0.09 (0.02)	0.09 (0.01)	0.14 (0.07)
December	0.09 (0.01)	0.09 (0.02)	0.08 (0.01)	0.09 (0.01)	0.16 (0.05)

* Numbers in parenthesis are the standard deviations of the monthly averages.

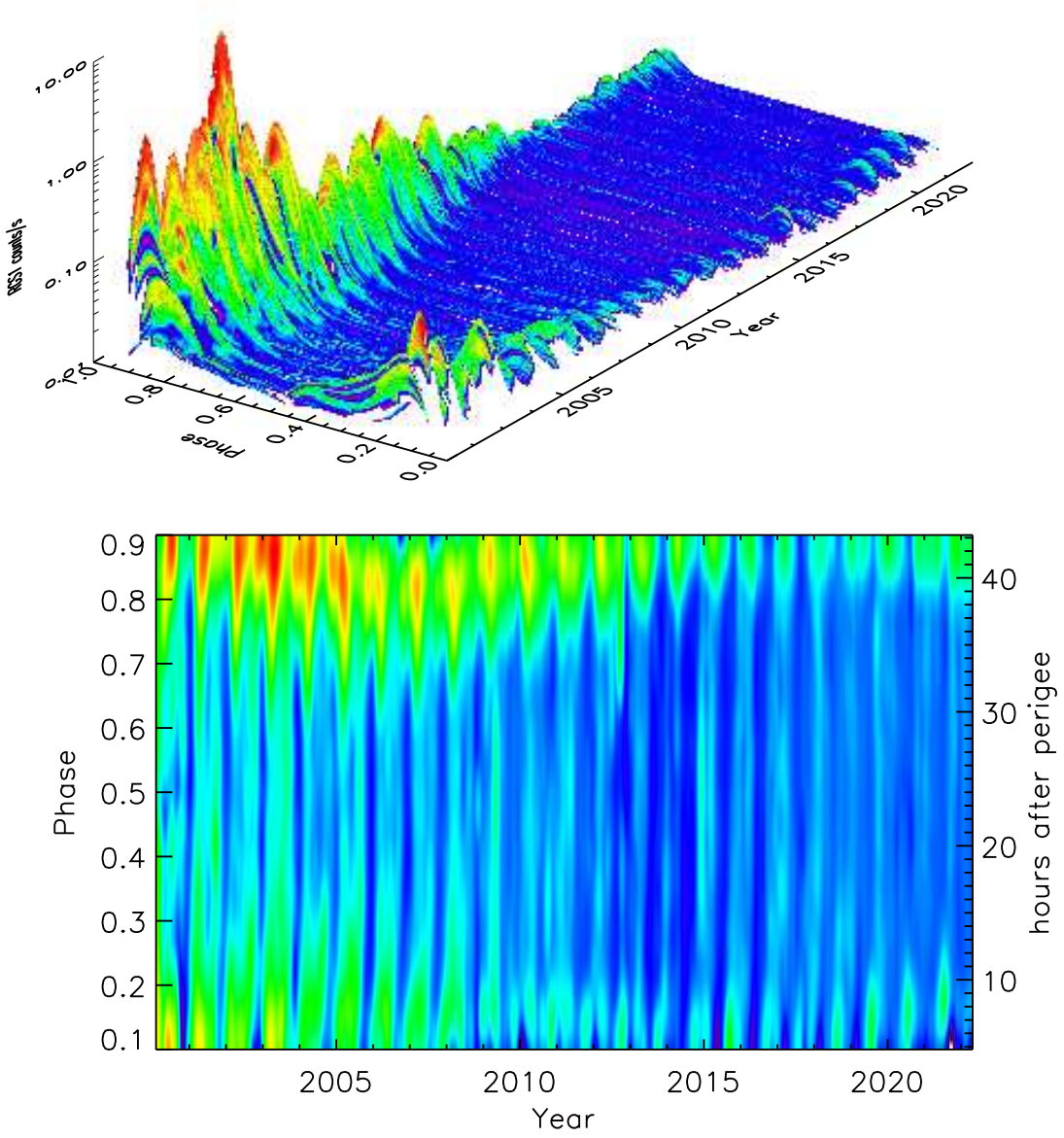

Figure 7: Top: Three-dimensional representation of the RGS background by date and by phase in the revolution; Bottom: Projection of the above surface in the Year/Phase plane.

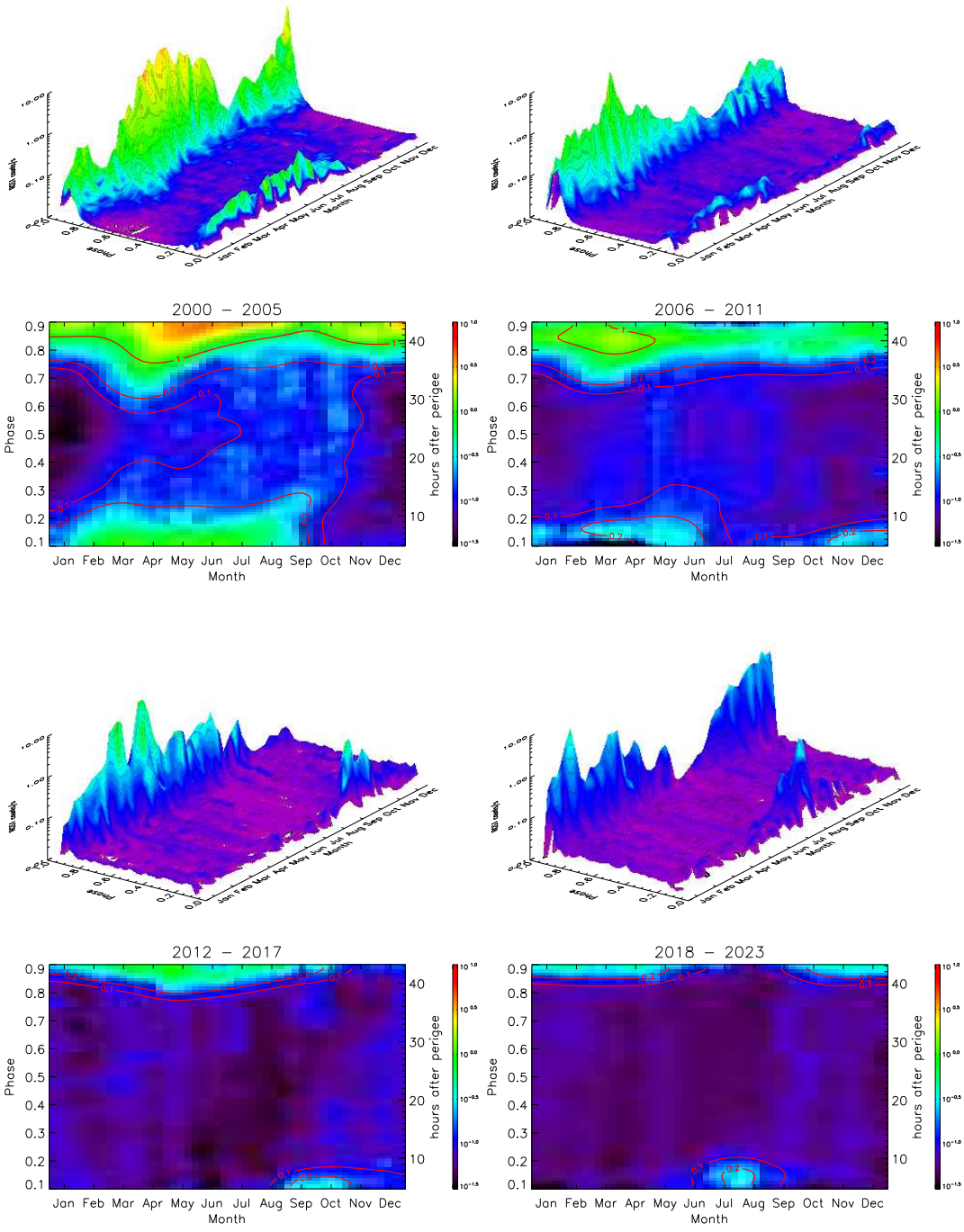

Figure 8: Behaviour of the RGS background by month (top left: until end 2005, top right: from 2006 to end 2011, bottom left: from 2012 to 2017, bottom right: from January 2017 until May 2023). In both figures the top panel is a representation of the RGS background by month and by phase in the revolution, and the bottom panel is the projection of the above surface in the Month/Phase plane, showing the contours corresponding to 0.1, 0.2 and 1 cts/s, defining the regions of low (dark blue), medium (light blue-green) and high (yellow-red) background.